Results in Materials 19 (2023) 100427

Contents lists available at ScienceDirect

Results in Materials

journal homepage: www.sciencedirect.com/journal/results-in-materials

Silver-based conductive coatings as lightning strike protection for composite aircraft

Anamaria Serbescu [a], David Brassard [a], Jean Langot [a], Etienne Gourcerol [a], Kambiz Chizari [a], Alexandra Desautels [b], Maxime Lapalme [b], Frédéric Sirois [a], Daniel Therriault [a,*]

[a] Polytechnique Montréal, P.O. Box 6079 Station Centre-Ville, Montréal, QC, H3C 3A7, Canada
[b] Bell Textron Canada Ltée, 12 800 Rue de l'Avenir, Mirabel, QC, J7J 1R4, Canada

ARTICLE INFO

Keywords:
Lightning strike protection
Composite materials
Electroless deposition
Conductive composites

ABSTRACT

Lightning strike protection of composite structures is an increasingly studied subject in the aerospace industry due to the need for finding novel protection solutions for low conductive composites. This work presents two silver-based lightning protective conductive coatings for potential replacement of expanded copper foil (ECF) as lightning strike protection (LSP). The first solution consists of an electroless method to produce silver-coated carbon fibres (SCCF). The SCCF are integrated as a sacrificial ply on a carbon fibre reinforced polymer (CFRP) panel with four different areal densities, using an epoxy-based primer or a PEDOT:PSS conductive ink as binder. The second solution is a silver-based commercial product consisting of a two-part epoxy with silver flakes, which acts as a sprayable thin coating beneath the paint layer.

The protected CFRP panels were covered with aerospace-grade paint for realistic finishing and were subjected to high impulse current strikes. All four conductive coatings containing SCCF exhibited around 45%–50% retention of flexural strength, although largely inferior to painted expanded copper foil's resistance to emulated lightning strikes. The silver-based commercial product showed 83% retention of flexural strength and 97% retention of effective bending modulus, with a comparable performance to the painted expanded copper foil. The resulting retention of flexural strength, the absence of severe damage to the structure, its versatility for complex geometries and the easy manufacturability of the silver-based commercial coating makes this approach a good candidate for the replacement of ECF as a solution for LSP.

1. Introduction

As global warming becomes an increasingly predominant issue in the modern world, many countries are introducing strict legislation to curb the growth of greenhouse gas emissions of many industries, including the aviation industry, which represented 2.4% of global greenhouse gas emissions in 2018 [1,2]. These countries have set their goal to reach carbon-neutral growth by 2035 and a net reduction of their emissions over the long term (2050) [3,4], following the Carbon Offsetting and Reduction Scheme for International Aviation (CORSIA) [5]. A major obstacle to the reduction of commercial aircraft emissions is the rising demand for passenger and freight post-pandemic transportation, and the carbon-neutral growth has not yet been reached [2]. The strict emission reduction requirements imposed to the industry force the aerospace companies to devise strategies and implement reduction plans such as converting their fleet to lighter and more efficient aircraft and using bio-sourced jet fuels [5]. Life cycle assessment demonstrated that the introduction of composite aircraft provides significant environmental benefits [6] and net negative emissions, even when taking into account the increased emissions from the manufacturing and decommissioning phases [7].

Composite structures however come with some limitations: they generally exhibit a much lower electrical conductivity than aluminum alloys, and unprotected elements are prone to sustaining significant damage when exposed to lightning strikes [8]. The ability to withstand lightning strikes without catastrophic failure is of capital importance for the airworthiness of a commercial aircraft, hence the resistance to lightning is an important design factor imposed by the Federal Aviation

* Corresponding author.
E-mail addresses: anamaria.serbescu@polymtl.ca (A. Serbescu), david.brassard@polymtl.ca (D. Brassard), jean.langot@polymtl.ca (J. Langot), etienne.gourcerol@polymtl.ca (E. Gourcerol), kambiz.chizari@polymtl.ca (K. Chizari), adesautels@bellflight.ca (A. Desautels), mlapalme01@bellflight.ca (M. Lapalme), f.sirois@polymtl.ca (F. Sirois), daniel.therriault@polymtl.ca (D. Therriault).

https://doi.org/10.1016/j.rinma.2023.100427
Received 22 January 2023; Received in revised form 18 March 2023; Accepted 30 July 2023
Available online 10 August 2023

Administration (FAA) [9], with recommended practices by the Society of Automotive Engineers (SAE) [10]. A solution that is widely used in the industry is the integration of a layer of expanded copper foil (ECF) on the outer surfaces of structures and assemblies prone to lightning strikes by co-curing them with the addition of resin on the composites [11]. ECF protective layers offer a good protection against damage from direct lightning strike, but add a significant weight penalty to composite structures due to their manufacturing process [11]. In addition, repairs of the outer layer after lightning events are complicated due to the need to correctly re-establish the conductive network in the copper foil [12]. Thus, despite the very good protection they offer, there is a need to search for new protective coatings to overcome the downsides of ECF. Conductive resin systems [13–15], nanofillers and buckypapers [16,17], conductive carbon fibre veils [18], metallic coatings [19,20], conductive fabric crimping [21,22], nickel-coated CF veils [23], conductive paints [24] and silver-coated carbon nanofibres [25,26] are just a few of the numerous solutions that are actively studied as alternatives to ECF. Silver being the only metal electrically and thermally more conductive than copper with respectively 6.2×10^7 S m^{-1} and 420 W m^{-1} K, it is considered as a very good candidate material for developing a LSP solution [27].

Cauchy et al. studied hybrid core-shell high aspect ratio carbon–silver nanofibres with a continuous silver coating, which effectively diverted the current strike with a conductivity of 2.5×10^5 S/m for a loading rate of 6.3% (vol.) [25]. Farahani et al. also studied the synthesis of silver nanoparticles, spread into a conductive ink and treated with an annealing process that resulted in a 4.2×10^{-3} Ω cm^{-2} [28] specific sheet resistivity. Diamanti et al. studied the synthesis of carbon nanotube (CNT) buckypapers (BP) for lightning strike protection by preparing hybrid buckypapers with silver nanoparticles and graphene nanosheets. The conductivity of the hybrid buckypaper reached 6.7×10^4 S/m for the biggest areal mass [29]. However, the application of such nanoscale solutions at an industrial scale would present significant risks for workers, and would require the development of conscientious methods of manufacturing as well as proper protection equipment and installations [30,31].

Previous work using silver-coated carbon nanofibres as a lightning strike protection system [25] showed good results, but has been only demonstrated on small panels so far and lacked the scalability required to cover large aerospace structures. In this paper, we present two silver-based conductive coatings for effective lightning strike protection without the health hazards of nanoscale solutions. The performance of these solutions are compared to that of ECF protected panels, which we consider as our baseline reference.

The first silver-based conductive coating consists of wet metallized milled carbon fibres integrated with PEDOT:PSS ink that acts as a sacrificial conductive coating on top of the carbon fibre reinforced polymer (CFRP) panels. PEDOT:PSS ink is used in thin conductive coatings, notably in the form of aqueous dispersion, solid film or hydrogel. It is a promising conductive polymer which could be used to create the basis of our network and potentially aid the conductive network of silver-coated carbon fibres (SCCF). The second conductive coating is a two-part epoxy coating with homogeneously dispersed silver flakes, known under the commercial name of Ultraconductive 4010/4011.

The emulated lightning strike experiments were performed on carbon fibre panels covered with the silver conductive coatings of different areal densities and coated with aerospace-grade paint. For reference panels, emulated lightning strikes were also conducted on painted CFRP panels and painted CFRP panels embedded with ECF. The efficiencies of the silver-based conductive coatings were assessed by measuring the retention of mechanical properties after an emulated lightning strike. The ultimate goal of this work is to obtain an efficient silver-based conductive coating for LSP that performs equally well or better than ECF, while being lighter.

2. Material and methods

2.1. Materials

2.1.1. Reference panels

Numerous quasi-isotropic composite panels were manufactured by autoclave consolidation of 8 plies of HTS40 3 k plain weave fabric from Teijin pre-impregnated with the 5276–1 epoxy from Solvay and assembled with a $[0°/45°]_{2s}$ sequence. The composite panels had a thickness of 1.69 mm and were cut into 30.5 cm × 30.5 cm (1 ft × 1 ft square samples) for emulated lightning strike experiments. The panels were coated with aerospace-grade paint with a thickness of 220 μm to serve as the unprotected reference (P-CFRP). Subsequently, ECF-protected benchmark panels were fabricated with an embedded expanded copper foil of 141 g m^{-2} and the addition of the surfacing film and resin with an areal density of around 191 g m^{-2}, amounting to a total integrated areal density of 322 g m^{-2}, hence the weight penalty aforementioned. The remaining CFRP panels were used for the integration of our conductive coatings, which their preparation is described in the experimental section.

2.1.2. Integration of the SCCF as a protective coating on CFRP panels

Prior to their deposition on the CFRP panels, the SCCF were filtered from their DI water solution with the filtering apparatus and then completely dried for 2 h at 90 °C in a vacuum oven to remove residual water. The SCCF plating process is described in the appendix.

2.1.2.1. Integration with primer. To improve the adhesion of the SCCF, a thin mist of MIL-PRF-23377 K, type I, class N epoxy primer from Hentzen was deposited on the panels with a 3 M Accuspray spray gun using a nozzle diameter of 1.4 mm. The dried SCCF were then evenly distributed on top of the panel with a 30 cm #100 sieve (opening size of 150 μm). A final coating of primer has been applied to seal the surface and prevent displacement of the SCCF. The panels were cured in an oven according to the specifications of the epoxy primer before being weighted and further tested.

2.1.2.2. Integration with conductive ink. The second method consisted of coating the surface-prepared panels with Ossila F HC Solar PEDOT:PSS (1.5% wt in aqueous solution), denominated as conductive ink. A thin coating was airbrushed with an ABEST gravity feed dual-action airbrush paint spray between each SCCF layers. After applying the PEDOT:PSS coating, the same sieving and sealing process as described above was used the integration with the primer. However, three surface densities of protective coatings were tested (not including the areal density of paint): 70 g m^{-2}, 150 g m^{-2} and 190 g m^{-2} with the $[\text{PEDOT:PSS/SCCF}]_{i\,=\,1,2,3}$ stacking sequence, where i is the number of layers in the stack. The repetition of layers thus adds more areal weight of the conductive coating on the panel. These conductive coatings and their stacking sequence are presented in Fig. 1, where each layer of each configuration is illustrated.

2.1.3. Integration of ultraconductive

The Ultraconductive 4010/4011 two-part epoxy commercial solution is a single layer sprayable coating that is certified for Zone 1A and Zone 2A, which represent the first return stroke zone and swept stroke zone defined in SAE's Aerospace Recommended Practices 5414 [10]. The product commercialized by LORD was produced and bought from Socomore to be integrated in our test plan as an alternative silver-based conductive coating but possesses a different conductive network due to the silver flakes that are integrated in the resin. The two products were shaken with a paint shaker for 10 min to disperse the silver flakes homogeneously within the mixture. This sprayable coating must to be applied on the tool mold of a composite piece or assembly before stacking pre-impregnated carbon cloths to form the protected composite

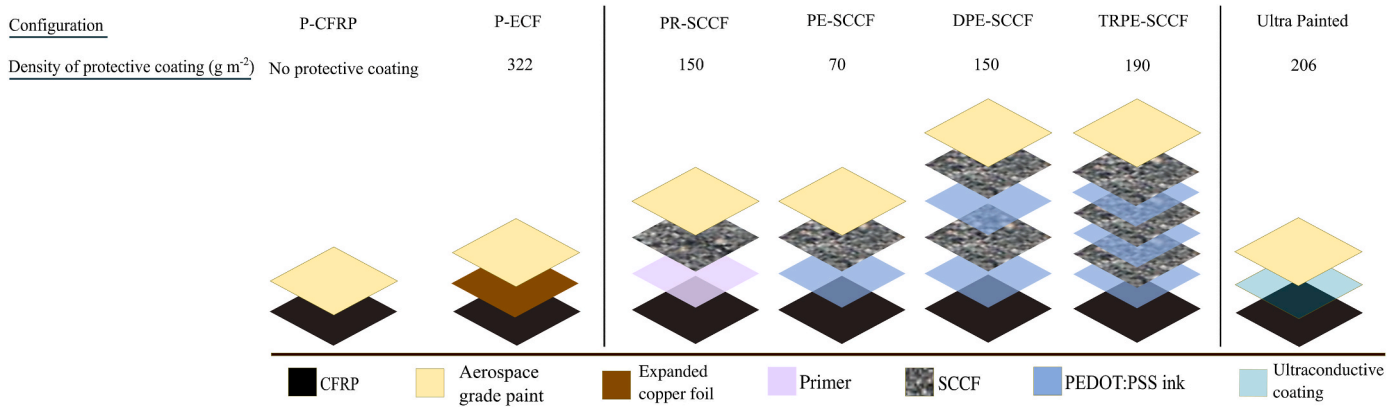

Fig. 1. Schematics of integrated layers with the areal densities of conductive coatings tested.

structure. The product was applied with a gravity gun, according to the manufacturer's recommendations, in order to form a uniform and wet appearing coating of 150 μm on the tool mold of the planar panels. The coating was then pre-baked 100 °C for 30 min in order to remove the solvent present in the product and to strengthen the coating. Then the pre-impregnated unidirectional carbon fibre fabrics were layed-up on top of the Ultraconductive layer and cured by autoclave moulding to form the protected CFRP panels. The panels were subsequently painted on the Ultraconductive side up, according to Bell Textron Canada Ltd's standard painting practices, and are referred to as Ultra Painted in this manuscript.

2.2. Electrical resistivity measurements

Measurements of the electrical resistivity of the coatings were made per ASTM F1711-96 [32] with an in-house four-point probe apparatus consisting of four spring-loaded pins distanced 5 mm apart, welded on a printed circuit board (PCB). A Keithley 6620 DC current source and a Keithley 2182A nanovoltmeter were used for current injection and voltage measurements respectively. These measurements were done on the solutions integrated on the panels before painting, since after the painting, it was not possible to establish anymore an electrical contact between the spring-loaded pins and the conductive coating to properly measure the sheet resistivity.

2.3. Emulated lightning strikes

Emulated lightning strikes with a peak current of ~ 40 kA were produced by the discharge of a bank of capacitors into a modified resistor-inductor (RL) circuit, as presented in Figure A1 in the appendix. Details about the development of this lightning strike emulator are given in the PhD thesis of R. Ponnada [33]. The emulator consists in a bank of capacitors that can be charged at a voltage up to 60 kV, a series resistor of 1 Ω, two graphite spheres that act as a spark gap and a free-wheeling diode. The current is injected in the samples with a 12.7 mm copper electrode with a tapered conical tip. The role of the diodes in parallel to the sample is to remove the oscillating behaviour of the underdamped RLC circuit to produce a current waveform similar to waveform A defined in the SAE ARP5412 standard [34]. The current is injected at the centre of the 30.5 cm × 30.5 cm panels. The sample is connected back to the capacitors by an aluminum frame pressed on the perimeter of the sample. The surface of the sample in contact with the aluminum frame is sanded to remove any paint or surface resin, which is essential to ensure good electrical contact with the aluminum frame. The current passing through the sample and the electrical voltage in the capacitors were recorded during the emulated lightning strikes with a Lecroy Wavesurfer 422 oscilloscope. The current was measured with a Rogowski Current Waveform Transducer CWT 600B from Power Electronic Measurements Ltd.

2.4. Mechanical testing

The flexural strength and modulus were evaluated by four-point bending test, according to the ASTM D6272 [35] standard. Degraded specimens were cut from the centre of the panels struck by lightning, with the specimen centred on the damaged section. The damaged coupons were solicited in bending, with the damaged side solicited in tension. In addition to specimens at the centre of the degraded panels, additional reference specimens were cut along the sides of the panels, far from the impacted zone. Each configuration had five damaged and undamaged coupons tested, except for the TRPE-SCCF conductive coating, which had only three damaged coupons, due to the high cost of the process and the challenge of integrating the coating at high areal density (190 g m^{-2}).

These damaged coupons were thus compared to the baseline coupons that were cut outside of the damaged impact area, in order to limit the variations of properties among panels with very similar conductive coatings. The maximum flexural strength and the effective bending modulus were measured using the Instron 1362 frame with MTS ReNew controller (load cell capacity of 5 kN, MTS TW-Elite software). The deflection of each coupon was recorded using a displacement gauge (model: MTS 632-06H-30).

Fig. 2a) shows the four-point bending test apparatus used to solicitate the damaged side in tension (damaged side up). Fig. 2b) shows a typical loading curve on the specimens during the four-point bending test. The load at the first maximum deflection (P) and the displacement at the first maximum deflection (D_{ef}) are used to calculate the maximum flexural strength and the effective bending stiffness. The results have been normalized for each sample tested. Fig. 2c) shows a photography of the apparatus with the installed deflectometer used to capture the displacement of the tested coupons during the four-point bending test.

2.5. Non destructive testing

Through-thickness and pulse-echo C-scans were carried-out with a TecScan's NDT Ultrasonic 12-axis gantry system. The panels were clamped vertically in the multi-axis gantry system. The gantry system uses a water jet coupling through-thickness transmission 5 MHz probe that scans the striked panels on the damaged side to assess the magnitude of subsurface damage and provide a quantitative value of the attenuation of the signal (due to defect detection) in decibels. The travel speed of the probe is 330 mm/s, the increment is 3 mm, which gives 110 passes to cover 100% of the panel's surface. The pattern is S-shaped, starting from the lower right corner to the upper left corner.

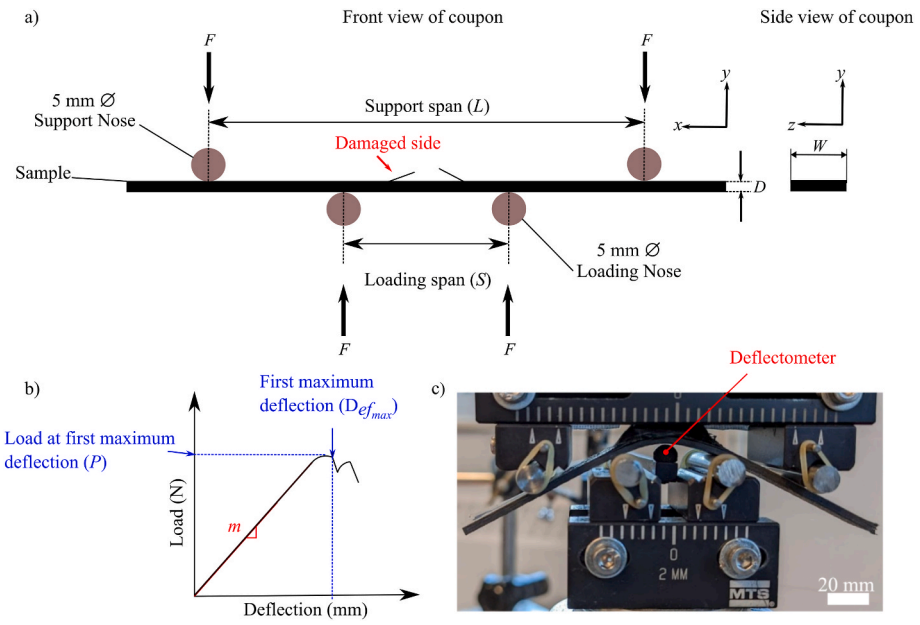

Fig. 2. Four-point-bending test schematics: a) Schematics of the loading span and support span with the damaged specimen side up, b) standard deflection-load curve, c) photography of the testing apparatus with the deflectometer.

3. Results

3.1. Optical and electron microscopy

Fig. 3 shows the SCCF at different magnification levels to assess quality of the electroless plating on the mCFs using the Tollen's reaction described in the experimental section. Fig. 3a) shows a view of an ensemble of SCCF, Fig. 3b) and c) demonstrate the continuity of the coating around the cross section and on the length of the carbon fibres. Fig. 3d) shows the measured thickness of the coating produced on the SCCF with scanning electron microscope (SEM). The silver coating thickness on each fibre, following the silvering process described above, was found to be about 0.35 µm.

To take advantage of the high electrical conductivity of silver, a continuously connected network of mCF is desirable. Silver seeds formation on the milled carbon fibres are undesirable. We rather seek an uniform coating that can help achieve the continuous network and to reduce contact resistance between individual mCFs to a minimum [25]. Fig. 3a)–3d) confirm the presence of continuous coatings on each mCFs. Fig. 3e) and f) respectively show the dispersion of the SCCF in the PR-SCCF sample and the sedimentation of the SCCF in the cured paint. Their dispersion through the paint could potentially reduce dielectric breakdown energy required, leading to lesser damage.

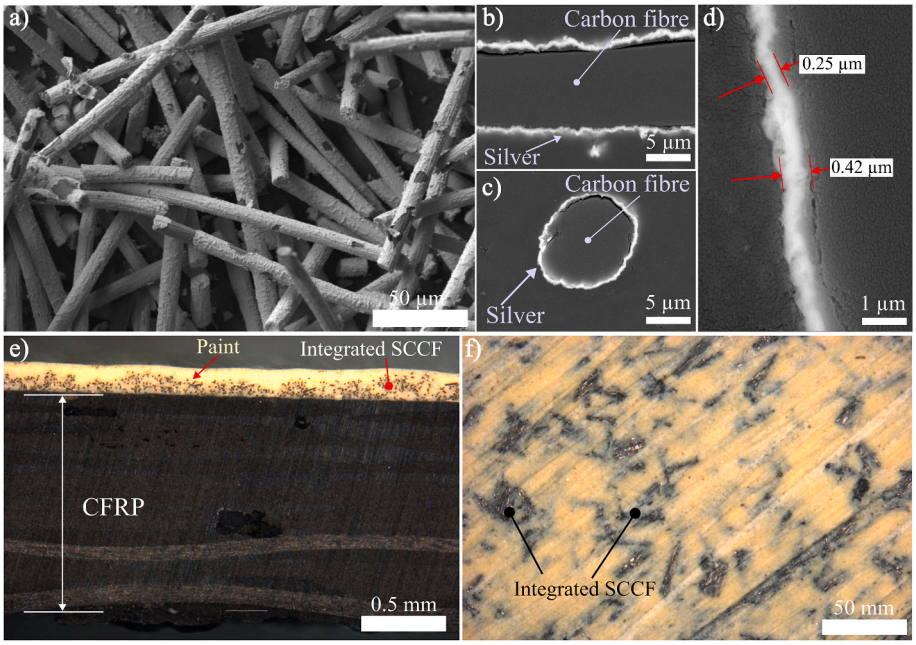

Fig. 3. Silver coated carbon fibres (SCCF) produced with the Tollen's reaction under Scanning Electron Microscopy (a–d). a) Silver coated milled carbon fibres, b) Side view of plated SCCF, c) Circular cross-section of SCCF, d) Coating thickness measurement of SCCF, e) Cross section view of integrated conductive coating PR-SCCF with paint (optical microscope), f) Sanded surface view of the perimeter of the panel (optical microscope).

3.2. Post-lightning strike results

Following the lightning strike tests, various measurements were performed to assess the damage induced by the strike. Both mechanical tests and non-destructive testing (NDT) methods were used. High impulse current strikes reflecting real lightning conditions induce many physical constraints that interact with each other in complex ways on the tested materials. Fig. 4 shows the current waveforms recorded on the various LSP-protected samples studied, as well as the respective decaying trend of the current for each sample. Generally, similar peak currents were reached for all samples. The slight variations are due to variation of initial charge of the capacitor bank of the lightning strike emulator (60 kV ± 5%). As a rule of thumb, the decaying time of each waveform is closely related to the sheet resistivity of the conductive coating. P-ECF and Ultra Painted samples were the most conductive ones and their currents decayed with the slowest rate: the time to half of the peak current amplitude was larger than that of the samples with less conductive coatings.

Table 1 shows the current strike parameters recorded, such as the peak current, the charge transfer and the action integral, defined as the integral of the square of the current with respect to time. The action integral is used to gauge the severity of the damage caused by the lightning current to the specimens' surfaces and is a representative value to quantify the amount of energy converting into heat in the specimens [36]. PR-SCCF, PE-SCCF, DPE-SCCF and TRPE-SCCF show a higher charge transfer as their sheet resistivity decreases. The same trend can be observed for their action integral. Ultra Painted shows the highest charge transfer and action integral among all silver-based conductive coatings. P-ECF, which is the most conductive solution obtained so far in term of sheet resistivity, shows the highest action integral among all and P-CFRP results in the lowest action integral and charge transfer among all panels tested. Note that all charge transfer and action integral values obtained in these tests are lower than what is required by the ARP5412 standard to certify a LSP solution (considering the scale-down current of 40 kA). This is partly explained by the higher surface resistance of the LSP solutions than that of traditional plain aluminum panels, as well as by some limitations of the in-house lightning strike emulator, which is slightly more sensitive to the samples' resistance than a full-scale current generator in a certification laboratory.

Fig. 5 shows in (i) a top view of the tested panels, in (ii) a cross section view of the point of impact, and in (iii) a C-scan view of the tested panels. In Fig. 5 row (i), PR-SCCF, PE-SCCF, DPE-SCCF and TRPE-SCCF all show significant area of fibre breakage. Ultra Painted shows no fibre breakage, with only sublimation of the paint and the Ultra-conductive coating. P-ECF shows virtually no visual damage. P-CFRP shows a significant area of damage around the entry point of the current strike, being the unprotected reference. Visual analysis of the top views also shows that all conductive coatings except P-ECF present paint sublimation following the current strike.

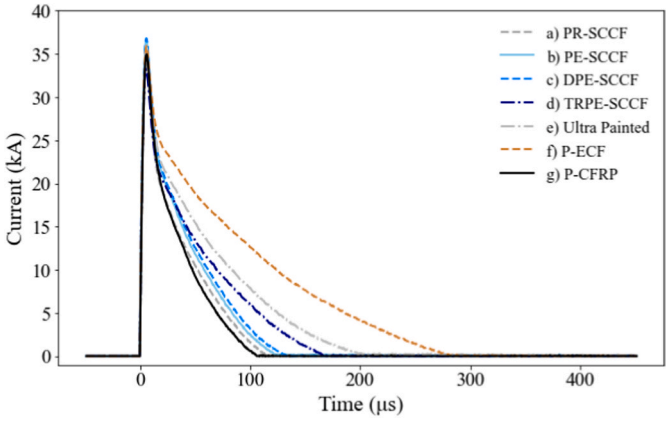

Fig. 4. Experimental current waveforms recorded for the different LS conductive coatings tested.

Table 1
Summary of electrical properties and lightning strike performances of all produced in this paper.

Sample	Peak current (kA)	Charge transfer (C)	Action Integral (A^2 s)	Sheet resistivity Ω/□
PR-SCCF	36.208	1.217	23.42×10^3	0.029
PE-SCCF	36.211	1.301	22.17×10^3	0.028
DPE-SCCF	35.948	1.376	24.98×10^3	0.021
TRPE-SCCF	33.811	1.402	25.37×10^3	0.020
Ultra Painted	33.435	1.741	27.91×10^3	0.012
P-ECF	36.201	2.907	50.15×10^3	0.007
P-CFRP	35.707	1.216	22.56×10^3	0.250

In Fig. 5 (ii) a) through d), significant delamination in the first two plies at the centre of current strike can be observed in all SCCF-based conductive coatings. Ultra Painted and P-ECF show no delamination at the point of impact, thus no distinct layers of the laminates have been separated from each other. P-CFRP shows delamination in the first two plies of the laminate, like the SCCF-based silver coatings. In Fig. 5 (iii), the C-scan with ultrasonic inspection a) through d) show that there is damage at the point of impact and irregularities in the conductive coatings over the whole surface of the panels. For the conductive coatings that have more than one SCCF layer, namely DPE-SCCF and TRPE-SCCF, the irregularity of thickness of the SCCF layers seem to appear as damage on the C-scan, but are in fact caused by the difficulty of integration of the subsequent SCCF and conductive ink layers. This seemingly observed damage around the point of impact (outside of the point of impact) is in fact attributed to the non uniformity of the coating thickness. It is to note that a constant thickness of paint on these more aerially dense conductive coatings was also difficult to achieve due to their manual integration, which contributed to the non-uniformity of the layers. Ultra Painted LSP shows slight damage at the point of entry of the impulse current, while P-ECF shows no damage in the underlying plies of the composite. P-CFRP shows substantial damage at the entry point.

3.3. Mechanical testing results

Fig. 6a) shows the retention of flexural strength of each conductive coating. PR-SCCF shows 25% lower retention of flexural strength than DPE-SCCF. Both conductive coatings possess the same areal density (150 g m^{-2}), which indicates the importance of using a conductive binder (PEDOT:PSS) that can effectively create a conductive network, leading to better shielding against lightning strike. The results of the mechanical tests on DPE-SCCF and TRPE-SCCF show that no remarkable improvement of retention of flexural strength was observed after two layers of SCCF coating. Indeed, TRPE-SCCF exhibits 3% less flexural strength retention than DPE-SCCF. Ultra Painted and P-ECF retained respectively 83% and 92% of their initial flexural strength. P-CFRP shows the most important loss of mechanical properties by retaining only 27% of its original flexural strength. The importance of proper protection stems in the need to avoid critical failure in the composite structures.

These results in flexural strength retention are in agreement with the cross sectional observation in Fig. 5 (ii), where all SCCF conductive coatings showed delamination in the first two plies, as well as fibre breakage, whereas Ultra Painted and P-ECF show no delamination or fibre breakage, which confirms their higher exhibited retention of mechanical properties. Fig. 6b) shows the charge recorded during the tests of every conductive coating. The least resistive coatings conduct more electrical charge from the emulated lightning strike. The samples with these coatings also retain better their flexural strength after impact. Fig. 6c) shows the effective bending modulus of each tested sample. The

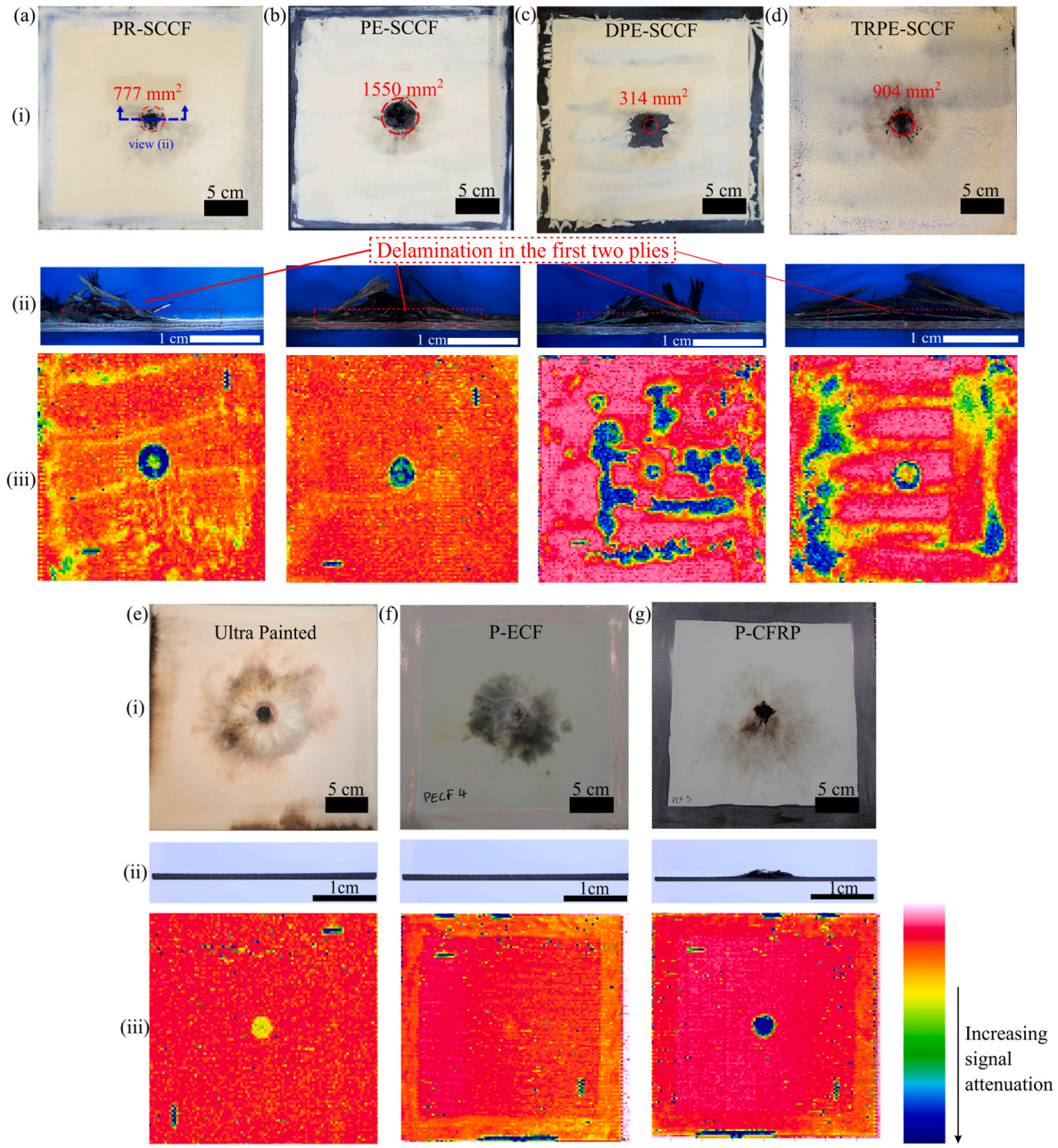

Fig. 5. Damage results on each tested conductive coating after lightning strike tests. (i) Photograph of the panel tested with red dotted line showing superficial fibre breakage; (ii) Optical image of the cross section of the point of impact showing delaminated plies; (iii) C-scan view of damaged panel where yellow to blue indicates progressive aggravation of damage and irregularity of coating for DPE-SCCF and TRPE-SCCF.

trend of effective bending modulus retention for each one is very similar to that of the retention of flexural strength. The retention of effective bending stiffness tends to be higher than retention of flexural strength due to Young's Modulus being less sensible to delamination [37].

Fig. 6d) shows the area of damage inflicted on the tested specimens. The silver-based solutions show big areas of damage compared to Ultra Painted and P-ECF. The area of damage of the conductive solutions is closely related to the retention of mechanical properties, as more aerially damaged specimens show lower retention of flexural strength and effective bending stiffness. Ultra Painted and P-ECF exhibit the least amount of damage respectively (628 mm^2 and 328 mm^2), which is correlated to their low sheet resistivity. The lightning damage is mainly due to the degradation and the evaporation of the resin of the CFRP structure caused by rapid heat generation from 1) the Joule heating created when the current goes through the matrix and 2) the heat associated to the electric arc that injects the current through dielectric materials such as resin and paint [33,38]. Severe damage can also be attributed to a acoustic shockwave and overpressure inside the laminate, leading to exploding damage [39].

4. Discussion

Our study aimed to compare a variety of silver-based conductive coatings on equal ground in conditions reflecting reality. Thereby, painted conductive coatings on CFRP panels were tested under emulated but realistic lightning strikes to see how well they would sustain this violent impact. The samples with SCCF conductive coatings (PR-SCCF, PE-SCCF, DPE-SCF and TRPE-SCCF) suffered substantial damage during lightning strike. Since the SCCF conductive coatings consisted of a thin layer of adhesive (primer or PEDOT:PSS) and a non-continuous coating,

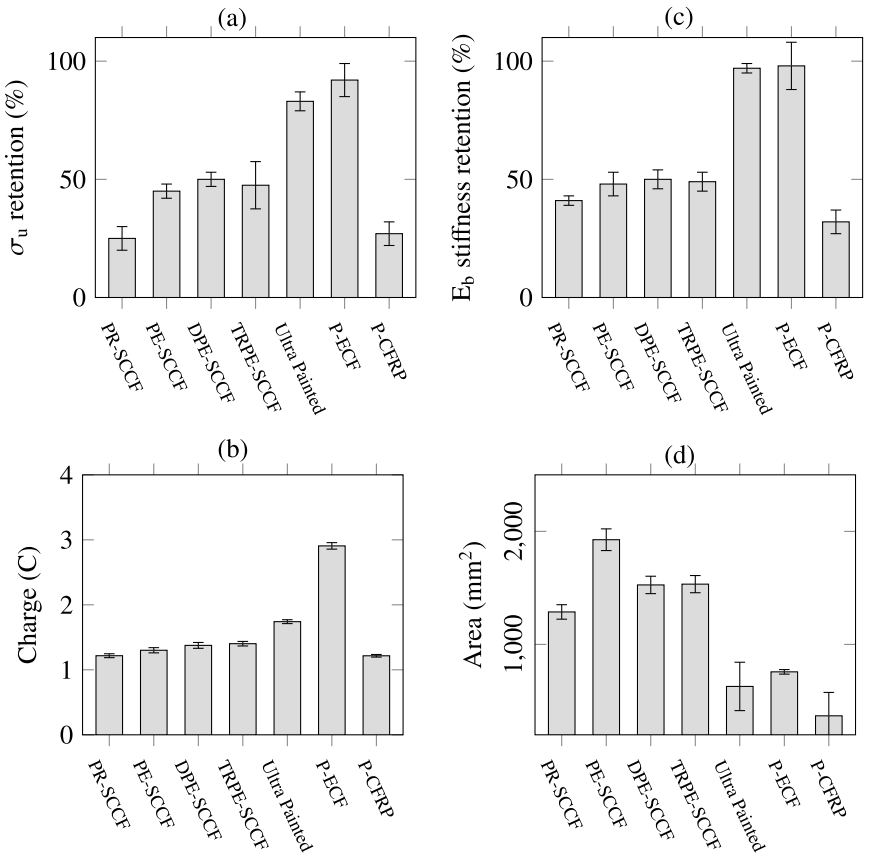

Fig. 6. a) Ultimate flexural strength retention (σ_u) (%), b) Charge transmitted to conductive coating during lightning strike, c) Effective bending stiffness retention (E_b) (%), d) Effective damaged area after lightning strike (mm^2).

the energy from the current strike may have rapidly vaporized the thin silver coating on the carbon fibres. In turn, this may have disrupted the thermal and electrical continuity of the coating, as the latent heat of vaporization of silver is 2.26 kJ g^{-1}, while it is 5.07 kJ g^{-1} for copper [27]. Therefore, the performances of the SCCF conductive coatings were inferior to that of the reference (and standard) P-ECF.

The Ultra Painted samples performed the best amongst the silver solutions with a retention of flexural strength of 83%, only 9% less than P-ECF. The loading of the silver flakes in the epoxy matrix lowered the resistivity of the epoxy resin to achieve a similar sheet resistivity than that of ECF integrated in resin. The observation of damage on the Ultra Painted samples shown in Fig. 5e) (iii) with ultrasonic inspection shows no visible sign of delamination or fibre breakage, and the area of damage is significantly less than all SCCF solutions, as per Fig. 6d). Ultra Painted thus provides a sufficiently conductive network to sustain thermal and electrical dissipation and could potentially be a satisfactory solution for a safe operation after a lightning strike.

5. Conclusion

The development of silver-based conductive coatings of composite panels as a solution for lightning strike protection was investigated in realistic conditions. The carbon fibre reinforced polymer (CFRP) panels with these experimental conductive coatings were produced and painted with aerospace-grade paint and tested under a modified A-waveform conformal to the SAE ARP5412 standard. The measurement of residual mechanical properties allowed for a quantitative assessment of the impact of damage and the structural integrity of the panels. The conductive coatings PE-SCCF, DPE-SCCF and TRPE-SCCF (Fig. 1) offered a similar retention of flexural strength (45%, 50% and 47.5% respectively), despite their gradual increase in areal density. A sheet resistivity of one order of magnitude more than that of P-ECF was reached with the silver-based conductive coatings, with at best a value of 0.02 Ω/□. The silver-based conductive coatings tested protected the composite panels better than the unprotected P-CFRP but still remained less performant than P-ECF.

Ultra Painted was the best candidate found. It offers similar protection than P-ECF, with 83% of retention in flexural strength and 97% of retention of effective bending stiffness. The manufacturing process of both silver-based conductive coatings (SCCF and Ultra Painted) allows for an adjustable areal density and has the potential to be implemented on geometries other than planar ones, and of larger areas.

The availability of an in-house lightning strike emulator setup provided us with a strong base of instrumentation and gave us good insights about the damage mechanisms of hybrid carbon-metal solutions. Further work on C-component behaviour (conformal to SAE ARP5412B) and electromagnetic shielding (EMI) should be conducted for the qualification of new silver-based lightning protection. Numerical modelling could also be a key tool to help us understand the mechanisms at work for the silver-based solutions presented in this paper.

Author statement

Anamaria Serbescu developed and scaled up the manufacturing method of the SCCF. Anamaria Serbescu manufactured the case study samples, thus all the silver-based conductive coatings on top of the composite panels. Etienne Gourcerol, Jean Langot and David Brassard participated in the emulated lightning strike test. Jean Langot performed the post-lightning strike mechanical retention tests. Anamaria Serbescu processed the experimental data, performed the analysis, drafted the manuscript, and designed the figures. Daniel Therriault, Frédéric Sirois and Kambiz Chizari were involved in planning and supervising the work.

Kambiz Chizari aided in interpreting the results and worked on the manuscript. Maxime Lapalme and Alexandra Desautels, our leading industrial partners, provided technical advice for materials and manufacturing. They also carried-out the fabrication of bare composite panels and the fabrication of expanded copper foil integrated panels. All authors discussed the results and commented on the manuscript.

Declaration of competing interest

The authors declare the following financial interests/personal relationships which may be considered as potential competing interests: Daniel Therriault reports financial support was provided by Bell Helicopter Textron Canada Ltd. Daniel Therriault reports financial support was provided by Natural Sciences and Engineering Research Council of Canada. There is no conflict of interest to declare.

Data availability

Data will be made available on request.

Acknowledgements

This work was supported by the Natural Sciences and Engineering Research Council of Canada (NSERC) under the alliance grant ALLRP 550062–20 with Bell Textron Canada Ltd. We would like to thank Bell Textron Canada Ltd for the manufacturing of the composite panels, the access to the C-scan equipment as well as their strong technical and financial support all along the project.

Appendix

7.1. Emulator Electrical Circuit

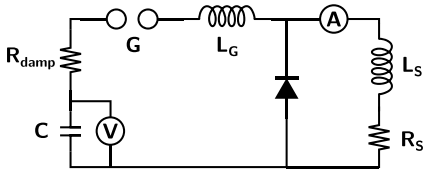

Fig. A1. Simplified electrical diagram of the lightning strike emulator: C represents the capacitors, R_s and L_s represent the resistance and inductance of the sample loop, L_G represents the inductance of the upstream circuit, G represents the sparkgap and A represents the Rogowski current probe.

7.2. Thermal imaging

A Telops MS M350 thermal camera was used to record the surface temperature on the coated side of the panels for 4.5 s, at a rate of 350 images per seconds. The thermal data could be recorded in a range of 20 °C–338 °C, limited by the type of optical filter used. The recording was synchronized with a light detector that was activated by the intense luminosity of the electric arc produced during the emulated lightning strike. The thermal data indicated when pyrolysis temperature was achieved. However due to the range of the filter, temperatures rapidly exceeded the 338 °C higher bound of the filter, leaving saturated pixels on the camera recordings. Thus, the observed rise and decay of temperature on the surface of the tested panels helped make a qualitative assessment of how conductive the coatings were but were not sufficient to conduct proper analysis.

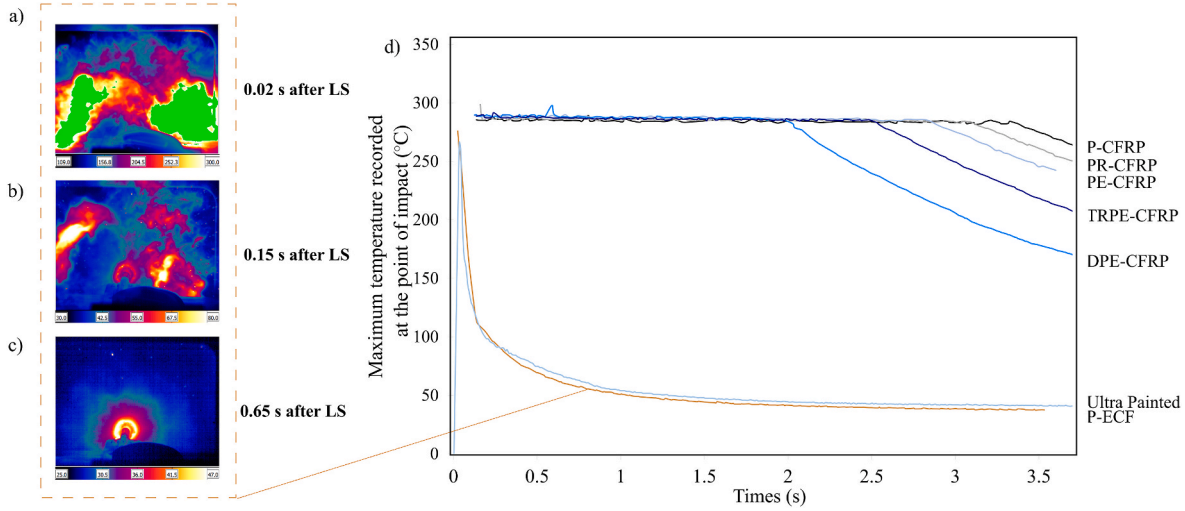

Fig. A2. Thermal profile of impacted silver-based conductive coatings a) 0.02 s after lightning strike, b) 0.15 s after lightning strike, c) 0.65 s after lightning strike, d) recorded temperature at centre of impact over time after lightning strike

7.3. Fabrication of Silver Coated Carbon Fibres (SCCF)

The silver deposition was performed on milled carbon fibres (mCF) PX-30 from Zoltek. The processed fibres had an average length of 150 μm and a diameter of 7 μm per company specifications.

The silvering process was based on the Tollen's reaction and adapted from the work of Cauchy et al. [25], but it has been scaled up for a large batch production of plated carbon fibres. The sensitization process was performed with stannous chloride dihydrate ($SnCl_2 \cdot H_2O$ 98%) and hydrochloric acid

(HCl ACS 36.5–38%) from Anachemia. The silvering process was performed with D-(+)-Glucose (dextrose), anhydrous ACS, potassium hydroxide (KOH ACS 45% weight fraction of H_2O), nitric acid (HNO_3 ACS 68–70%) from VWR BDH Chemicals, denatured reagent Alcohol 94–96% from Macron Fine Chemicals, silver nitrate ($AgNO_3$ ACS) and ammonium hydroxide (NH_4OH ACS 28%) from Anachemia.

7.3.1. Sensitization process

The sensitization of the mCF prepared the surface for the deposition of silver (Ag). This step produces a uniform coating of tin (Sn) on the surface of the mCF that facilitates the adhesion of the silver salts during the silvering process.

The sensitization was performed in a 1 l beaker with a Sonics ultrasonic processor matched to a probe with a 12 mm straight tip. The treated mCF were filtered out of the treatment solution with a 90 mm diameter vacuum membrane filtration apparatus with a capacity of 4 l. To process a batch of 5 g of raw mCF, 8 g of $SnCl_2 \cdot H_2O$ were mixed in 800 ml of deionized (DI) water to obtain a sensitization solution concentration of 10 g l^{-1}. With the addition 3 ml of HCl, we obtained a solution with a concentration of 160 mmol of HCl. The raw mCF (5 g) were then dispersed in the sensitization solution and sonicated during 20 min while keeping the solution below 45 °C. The functionalized mCF were subsequently rinsed at least 5 times in a vacuum filtration apparatus with DI water until a neutral pH was reached and no Cl^- ions were detected, while never letting the mCF dry.

During the rinsing step, the presence of Cl^- ions can be determined by adding aqueous silver nitrate. If Cl^- ions are present in solution, silver chloride (AgCl) precipitates and the solution turns cloudy.

7.3.2. Silvering process

The silvering process was based on an electroless deposition of silver salts on the sensitized mCF. The reducing solution (A) and the Tollen's reagent (B) were prepared separately before the silver deposition. All the reported masses and volumes of reagents have been calculated for the treatment of the initial 5 g of raw mCF sensitized during the sensitization step.

Reducing solution (A). The reducing solution was based on a dextrose solution with ethanol. It was produced by preparing a 20% w/w dextrose solution by dissolving 72 g of dextrose in 288 g of DI water and by adding 75 ml of denatured ethanol into 360 g of the dextrose mother solution. A larger volume of the reducing solution can be prepared ahead of time and used as needed.

Tollen's reagent (B). The Tollen's reagent is a solution of diamminesilver(I+) coordination complex that is later reduced by the reducing solution (A) to form silver salts. The Tollen's reagent was always freshly prepared before the silvering process when needed by combining 2 ml of KOH (ACS 45%) with 369 ml of DI water to obtain a 6.2×10^{-2} M solution. A mass of 25.5 g of $AgNO_3$ was mixed into 360 ml of DI water to reach a 0.5 M solution (89.94 g l^{-1}). Under magnetic stirring, 10 ml of the 6.2×10^{-2} M KOH solution were added into the 0.5 M $AgNO_3$ solution: the resulting solution turned cloudy and brown upon the reaction. Finally, 10 ml of NH_4OH were added dropwise until the solution became transparent again.

Silvering deposition process. Prior to the usual step of reducing solution A with solution B, sensitized mCF were added to solution A to promote galvanic exchange of silver ions on their surface. This step improved the uniformity of the silver coating obtained during the silvering process [39]. The plating process took place in a 1 l beaker that was prealably cleaned by swirling HNO_3 on the inside and rinsing with DI water until neutral pH was reached. The 5 g of sensitized mCF were put to rest in the Tollen's reagent for 5 min to let the galvanic exchange between tin and silver occur. The reducing solution (A) was poured into the beaker followed by Tollen's reagent (B) mixed with the sensitized mCF. The reaction was left to procede for 25 min under magnetic stirring at 650 rpm. After the silvering reaction had completed, the fibres were rinsed out in a vacuum filtration apparatus with a pore size of 5 μm with DI water until the solution became neutral. The SCCF were stored in DI water for future use.

References

[1] M. Klöwer, M. Allen, D. Lee, S. Proud, L. Gallagher, A. Skowron, Quantifying aviation's contribution to global warming, Environ. Res. Lett. 16 (2021), 104027, https://doi.org/10.1088/1748-9326/ac286e.

[2] J. Overton, Issue Brief | the Growth in Greenhouse Gas Emissions from Commercial Aviation (2019, Revised 2022), Environmental and Energy Study Institute, 2022.

[3] TC TC, Canada's Action Plan to Reduce Greenhouse Gas Emissions from Aviation, 2012. ISBN 9781100205434.

[4] Federal Aviation Administration, Aviation Environmental and Energy Policy Statement, 2012. https://www.faa.gov/sites/faa.gov/files/about/office_org/headquarters_offices/apl/FAA_EE_Policy_Statement.pdf.

[5] CORSIA, Carbon Offsetting and Reduction Scheme for International Aviation Implementation Plan, 2019.

[6] A.J. Timmis, A. Hodzic, L. Koh, M. Bonner, C. Soutis, A.W. Schäfer, et al., Environmental impact assessment of aviation emission reduction through the implementation of composite materials, Int. J. Life Cycle Assess. 20 (2) (2015) 233–243, https://doi.org/10.1007/s11367-014-0824-0.

[7] A.J. Beck, A. Hodzic, C. Soutis, C.W. Wilson, Influence of implementation of composite materials in civil aircraft industry on reduction of environmental pollution and greenhouse effect, IOP Conf. Ser. Mater. Sci. Eng. 26 (1) (2011), https://doi.org/10.1088/1757-899X/26/1/012015.

[8] Q. Dong, G. Wan, Y. Guo, L. Zhang, X. Wei, X. Yi, et al., Damage analysis of carbon fiber composites exposed to combined lightning current components D and C, Compos. Sci. Technol. 179 (17923) (2019) 1–9, https://doi.org/10.1016/j.compscitech.2019.04.030.

[9] F.A. Association, Transport Airplane and Engine Issue Area Electromagnetic Effects Harmonization Working Group. Task 2 – Lightning Protection Requirements, 2012.

[10] S.A.E. Aerospace, Aircraft Lightning Zoning ARP5414, 2018.

[11] M. Gagné, D. Therriault, Lightning strike protection of composites, Prog. Aero. Sci. 64 (2014) 1–16, https://doi.org/10.1016/j.paerosci.2013.07.002.

[12] H. Kawakami, P. Feraboli, Lightning strike damage resistance and tolerance of scarf-repaired mesh-protected carbon fiber composites, Compos Part A Appl Sci Manuf 42 (2011), https://doi.org/10.1016/j.compositesa.2011.05.007. https://linkinghub.elsevier.com/retrieve/pii/S1359835X11001448.

[13] Y. Hirano, T. Yokozeki, Y. Ishida, T. Goto, T. Takahashi, D. Qian, et al., Lightning damage suppression in a carbon fiber-reinforced polymer with a polyaniline-based conductive thermoset matrix, Compos. Sci. Technol. 127 (2016) 1–7, https://doi.org/10.1016/j.compscitech.2016.02.022.

[14] A. Katunin, K. Krukiewicz, R. Turczyn, P. Sul, K. Dragan, Lightning strike resistance of an electrically conductive CFRP with a CSA-doped PANI/epoxy matrix, Compos. Struct. 181 (2017) 203–213, https://doi.org/10.1016/j.compstruct.2017.08.091.

[15] V. Kumar, T. Yokozeki, T. Okada, Y. Hirano, T. Goto, T. Takahashi, et al., Polyaniline-based all-polymeric adhesive layer: an effective lightning strike protection technology for high residual mechanical strength of CFRPs, Compos. Sci. Technol. 172 (2019) 49–57. https://linkinghub.elsevier.com/retrieve/pii/S0266353818324904.

[16] J.H. Han, H. Zhang, M.J. Chen, D. Wang, Q. Liu, Q.L. Wu, et al., The combination of carbon nanotube buckypaper and insulating adhesive for lightning strike protection of the carbon fiber/epoxy laminates, Carbon N Y 94 (2015) 101–113, https://doi.org/10.1016/j.carbon.2015.06.026.

[17] J. Zhang, X. Zhang, X. Cheng, Y. Hei, L. Xing, Z. Li, Lightning strike damage on the composite laminates with carbon nanotube films: protection effect and damage mechanism, Composites, Part B 168 (March) (2019) 342–352, https://doi.org/10.1016/j.compositesb.2019.03.054.

[18] Z.J. Zhao, G.J. Xian, J.G. Yu, J. Wang, J.F. Tong, J.H. Wei, et al., Development of electrically conductive structural BMI based CFRPs for lightning strike protection, Compos. Sci. Technol. 167 (March) (2018) 555–562, https://doi.org/10.1016/j.compscitech.2018.08.026.

[19] H. Che, M. Gagné, P.S. Rajesh, J.E. Klemberg-Sapieha, F. Sirois, D. Therriault, et al., Metallization of carbon fiber reinforced polymers for lightning strike protection, J. Mater. Eng. Perform. 27 (10) (2018) 5205–5211, https://doi.org/10.1007/s11665-018-3609-y.

[20] S.M.R. Ponnada, F. Sirois, D. Therriault, Damage response of composites coated with conducting materials subjected to emulated lightning strikes, Mater. Des. 139 (2018) 45–55, https://doi.org/10.1016/j.matdes.2017.10.017.
[21] J. Rehbein, P. Wierach, T. Gries, M. Wiedemann, Improved electrical conductivity of NCF-reinforced CFRP for higher damage resistance to lightning strike, Compos Part A Appl Sci Manuf 100 (2017) 352–360, https://doi.org/10.1016/j.compositesa.2017.05.014.
[22] D.M. Lombetti, A.A. Skordos, Lightning strike and delamination performance of metal tufted carbon composites, Compos. Struct. 209 (February 2018) (2019) 694–699, https://doi.org/10.1016/j.compstruct.2018.11.005.
[23] Y. Guo, Y. Xu, Q. Wang, Q. Dong, X. Yi, Y. Jia, Eliminating lightning strike damage to carbon fiber composite structures in Zone 2 of aircraft by Ni-coated carbon fiber nonwoven veils, Compos. Sci. Technol. 169 (17923) (2019) 95–102, https://doi.org/10.1016/j.compscitech.2018.11.011.
[24] B. Zhang, V.R. Patlolla, D. Chiao, D.K. Kalla, H. Misak, R. Asmatulu, Galvanic corrosion of Al/Cu meshes with carbon fibers and graphene and ITO-based nanocomposite coatings as alternative approaches for lightning strikes, Int. J. Adv. Manuf. Technol. 67 (5–8) (2013) 1317–1323, https://doi.org/10.1007/s00170-012-4568-3.
[25] X. Cauchy, J.E. Klemberg-Sapieha, D. Therriault, Hybrid carbon–silver nanofillers for composite coatings with near metallic electrical conductivity, Adv. Eng. Mater. 20 (12) (2018) 1–8, https://doi.org/10.1002/adem.201800541.
[26] X. Cauchy, J.E. Klemberg-Sapieha, D. Therriault, Synthesis of highly conductive, uniformly silver-coated carbon nanofibers by electroless deposition, ACS Appl. Mater. Interfaces 9 (2017) 29010–29020, https://doi.org/10.1021/ACSAMI.7B06526/SUPPL_FILE/AM7B06526_SI_001.PDF. https://pubs.acs.org/doi/abs/10.1021/acsami.7b06526.
[27] U. of Texas, Chemistry 301, data & tables. Tech. Rep.; ? ? ? ?. https://ch301.cm.utexas.edu/data/index.php.
[28] R. Dermanaki Farahani, M. Gagne, J.E. Klemberg-Sapieha, D. Therriault, Electrically conductive silver nanoparticles-filled nanocomposite materials as surface coatings of composite structures, Adv. Eng. Mater. 18 (7) (2016) 1189–1199, https://doi.org/10.1002/adem.201500544.
[29] E. Diamanti, B. Falzon, S. Hawkins, Comparative study of electrical properties of different carbon nanotube buckypaper for lightning strike protection applications, in: International Conference on Composite Materials (ICCM21) ; Conference Date: 21-08-2017 through 25-08-2017, 2017.
[30] H. Becker, F. Herzberg, A. Schulte, M. Kolossa-Gehring, The carcinogenic potential of nanomaterials, their release from products and options for regulating them, Int. J. Hyg Environ. Health 214 (3) (2011) 231–238, https://doi.org/10.1016/j.ijheh.2010.11.004. https://www.sciencedirect.com/science/article/pii/S143846391000146X.
[31] M. Tanaka, Ki Inoue, A. Shimada, T. Mimura, H. Takano, Effects of repeated pulmonary exposure to carbon nanotubes on lung function, Toxicol. Environ. Health Sci. 11 (2019) 120–124, https://doi.org/10.1007/s13530-019-0396-2.
[32] ASTM, ASTM F1711-96, Standard Practice for Measuring Sheet Resistance of Thin Film Conductors for Flat Panel Display Manufacturing Using a Four-Point Probe, 2017.
[33] P. Rajesh, Response of Composite Panels with Conductive Coatings Submitted to Emulated Lightning Strikes. Phd thesis; École Polytechnique de Montréal, 2017. https://publications.polymtl.ca/2751/.
[34] S.A.E. Aerospace, ARP5412 REV. B Aircraft Lightning Environment and Related Test Waveforms, 2013.
[35] ASTM D6272-17, Standard Test Method for Flexural Properties of Unreinforced and Reinforced Plastics and Electrical Insulating Materials by Four-Point Bending.
[36] Y. Li, R. Li, L. Lu, X. Huang, Experimental study of damage characteristics of carbon woven fabric/epoxy laminates subjected to lightning strike, Compos. Appl. Sci. Manuf. 79 (2015) 164–175, https://doi.org/10.1016/j.compositesa.2015.09.019.
[37] Z. Liu, P. Li, N. Srikanth, Effect of delamination on the flexural response of [+45/45/0]2s carbon fibre reinforced polymer laminates, Compos. Struct. 209 (October 2018) (2019) 93–102, https://doi.org/10.1016/j.compstruct.2018.10.049.
[38] A. Bigand, Damage Assessment on Aircraft Composite Structure Due to Lightning Constraints, 2020. https://oatao.univ-toulouse.fr/25158/1/Bigand_25158.pdf.
[39] E. Rupke, Lightning Direct Effects Handbook. Tech. Rep.; AGATE - Advanced General Aviation Transport Experiments, 2002. https://skybrary.aero/sites/default/files/bookshelf/3352.pdf.